

# The Importance of Stacking and Coordination for Li, Na, and Mg Diffusion and Intercalation in $\text{Ti}_3\text{C}_2\text{T}_2$ MXene

Jacob Hadler-Jacobsen and Sondre Kvalvåg Schnell\*

The 2D layered  $\text{Ti}_3\text{C}_2\text{T}_2$  MXene is known for its diverse chemistry and has been investigated as potential anode and cathode in Li, Na, and Mg batteries.  $\text{Ti}_3\text{C}_2\text{T}_2$  layers can stack in at least two different ways depending on the termination group chemistry. In addition, stacking and termination groups influence the diffusivity and energy of ions intercalated in the MXene. How stacking influences the diffusivity, and how intercalated ions influence the stacking stability are not fully understood. In this study, density functional theory simulations explore Li, Na, and Mg ions intercalated in  $\text{Ti}_3\text{C}_2\text{T}_2$  stacked in four different ways; two are experimentally verified, and previously discussed in literature, and two with limited experimental evidence. It is shown that the stacking can reduce diffusion by 8–20 orders of magnitude. It is also explained how the termination group chemistry and the intercalated Li/Na/Mg ions change the relative stability of the stackings. The stacking's influence on diffusion properties is explained by examining the coordination of the ions at different points along the migration path. It is suggested that  $\text{Ti}_3\text{C}_2\text{T}_2$  with significant fluorine termination can be well-suited for especially Na anode use, and regardless of termination is unsuited as Mg cathode.

Cheng et al.<sup>[1]</sup> achieved a capacity equivalent to  $\text{Li}_{0.7}\text{Ti}_3\text{C}_2\text{T}_2$  (100 mAh g<sup>-1</sup> capacity after 200 cycles at 1C giving  $\approx 100$  mA g<sup>-1</sup>), and Wang et al.<sup>[2]</sup> achieved a capacity equivalent of  $\approx \text{Na}_{0.5}\text{Ti}_3\text{C}_2\text{T}_2$  (70 mAh g<sup>-1</sup> capacity after 1000 cycles at 200 mA g<sup>-1</sup> giving  $\approx 3$ C in rate). It has also been shown in tunnelling electron microscope (TEM) that several layers of Na can intercalate in some cases,<sup>[2]</sup> allowing more than one Na for every formula atom level unit at the atomic level, i.e.,  $\text{Na}_x\text{Ti}_3\text{C}_2\text{T}_x$ . Mg, on the other hand, is known to be a challenging metal for battery applications, with slow diffusion, troublesome electrolyte–electrode kinetics and problems with proton intercalation and electrolyte decomposition,<sup>[5–7]</sup> and has only demonstrated the equivalent of  $\text{Mg}_{0.004}\text{Ti}_3\text{C}_2\text{T}_2$  ( $\approx 1$  mAh g<sup>-1</sup>, 25 cycles) when tested on micron sized  $\text{Ti}_3\text{C}_2\text{T}_x$ .<sup>[3]</sup> Employing spacer groups to increase interlayer distance<sup>[8]</sup> and/or nano sizing the MXene<sup>[9,10]</sup> has shown increased

capacities, but it can be difficult to determine whether these capacities are due to reversible  $\text{Mg}^{2+}$  intercalation, or due to surface reactions, proton intercalation and/or cointercalation of electrolyte as with the case of  $\text{MgCl}^+$  intercalation.<sup>[5,6,11]</sup>


Much is unknown about MXene interlayer chemistry. The termination groups of the HF etched  $\text{Ti}_3\text{C}_2\text{T}_x$ , likely consists of O, OH, and F and the ratio between these species and the total number of them can be influenced by synthesis<sup>[12]</sup> and postsynthesis treatment.<sup>[13]</sup> By employing advanced techniques involving molten salts, it has been shown the termination groups can also include Cl, Br, S, Se, and Te.<sup>[14,15]</sup> While  $\text{Ti}_3\text{C}_2\text{T}_x$  is the best known MXene and by far most studied,<sup>[4]</sup> other MXenes have been investigated for energy storage applications as well.<sup>[16]</sup>

The interlayer chemistry can lead to different stacking-orders of MXene 2D layers, with implications for intercalation energies and kinetics. There have been theoretical investigations on  $\text{Ti}_3\text{C}_2\text{T}_2$  MXene stacked in two distinct ways.<sup>[17–20]</sup> The two stackings previously investigated are both AB-type and shown as ZZ-prismatic and ZZ-octahedral in Figure 1. They are labeled ZZ in this work due to their characteristic zig-zag pattern. For the octahedral stackings, the termination groups are arranged so that octahedrons can be drawn between the layers, and for the prismatic stackings trigonal prisms can be drawn between the layers. The ZZ-prismatic stacking can be seen in TEM images in the work of Wang et al.,<sup>[2]</sup> both with and without Na intercalated, and in the work of Cheng et al.<sup>[1]</sup> for MXene post treated with  $\text{NH}_3$ . In the work of Kamysbayev et al.,<sup>[14]</sup> they show

## 1. Introduction

MXenes, an expanding group of 2D materials typically derived from MAX-phases, have been investigated for use in both Li-, Na-, and Mg-battery applications.<sup>[1–3]</sup> The most studied MXene,<sup>[4]</sup> namely  $\text{Ti}_3\text{C}_2\text{T}_x$ , is shown in Figure 1 for the fully terminated case of  $\text{Ti}_3\text{C}_2\text{T}_2$ . It has been investigated primarily for cathode applications for Mg batteries,<sup>[3]</sup> and anode applications for Li,<sup>[1,2]</sup> and Na-batteries,<sup>[2]</sup> illustrating the versatility of the MXene, and the potential to use the same material for different applications. Reversible intercalation has been demonstrated for both Li and Na in pristine HF-etched  $\text{Ti}_3\text{C}_2\text{T}_x$ .<sup>[2]</sup> The capacity depends on the charge/discharge rate and other factors, but as an example

J. Hadler-Jacobsen, S. K. Schnell  
Department of Materials Science and Engineering  
Norwegian University of Science and Technology  
NTNU  
Trondheim NO-7491, Norway  
E-mail: sondre.k.schnell@ntnu.no

 The ORCID identification number(s) for the author(s) of this article can be found under <https://doi.org/10.1002/admi.202200014>.

© 2022 The Authors. Advanced Materials Interfaces published by Wiley-VCH GmbH. This is an open access article under the terms of the Creative Commons Attribution License, which permits use, distribution and reproduction in any medium, provided the original work is properly cited.

DOI: 10.1002/admi.202200014

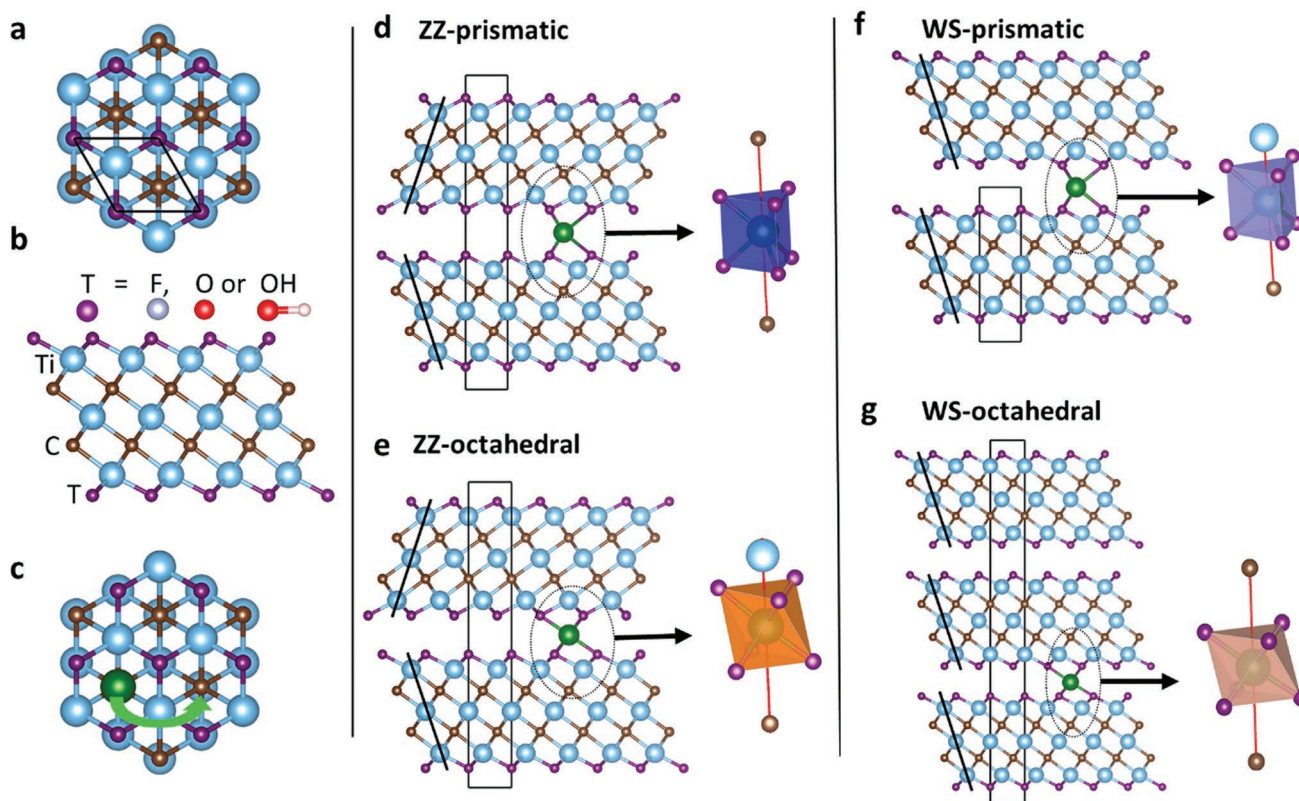


**Figure 1.** a)  $\text{Ti}_3\text{C}_2\text{T}_2$  seen along the  $c$ -axis, with the unit cell drawn. b) One layer of  $\text{Ti}_3\text{C}_2\text{T}_2$  along the  $a$ -axis with labeling of the elements. The termination groups studied in this work can be either F, O, or OH. c) The minimum energy path of Li/Na/Mg (green sphere) on the bottom layer in d–g), as seen along the  $c$ -axis. d–g) Four different ways to stack  $\text{Ti}_3\text{C}_2\text{T}_2$ , and how the resulting coordination for intercalated Li/Na/Mg becomes either octahedral or trigonal prismatic. The thick black lines in d–g) illustrates how the MXene layers “tilt” either a whip stitch (WS) manner or in a zigzag manner (ZZ). The simulation cell/unit cell is drawn with black lines in a) and d–g), illustrating that d) and e) have AB-type stacking, f) has AA-type, and g) has ABC-type.

figures of the of Cl, Br, and S terminated  $\text{Ti}_3\text{C}_2\text{T}_2$  structure, all with ZZ-prismatic stacking, even though TEM images in the same work seem to show a mixture of ZZ-prismatic and ZZ-octahedral stacking. Mixed or unclear stacking can also be seen in ref. [15] and ref. [21] and has also been predicted to be present for at least some surface termination compositions from both our previous density functional theory (DFT) study<sup>[20]</sup> and a study combining neutron diffraction data and multilevel modeling.<sup>[12]</sup> ZZ-octahedral stacking on the other hand, seems to be present in the work of Cheng et al.<sup>[1]</sup> for pristine  $\text{Ti}_3\text{C}_2\text{T}_x$  and for Al intercalated  $\text{Ti}_3\text{C}_2\text{T}_2$  in the work of Wang et al.<sup>[2]</sup>

It has been shown in two theoretical studies that differences in stacking decrease diffusion by orders of magnitude for both Li in  $\text{Ti}_2\text{C}_2\text{O}_2$ <sup>[22]</sup> and Li, Na, and Mg in our previous work on  $\text{Ti}_3\text{C}_2\text{O}_2$ .<sup>[20]</sup> For Li in  $\text{Ti}_2\text{C}_2\text{O}_2$ , Thygesen et al.<sup>[22]</sup> labeled the stackings simply AB and AA. The AA stacked  $\text{Ti}_2\text{CO}_2$  would be of ZZ-prismatic type following the terminology of this work. Special care should be taken when talking about AB-stackings, as there is more than one unique way to stack in an AB fashion for MXenes. Thygesen et al.<sup>[22]</sup> did not distinguish between these but judging from a figure in their work it appears that their AB stacking is what is labeled WS-octahedral in this work. In our previous work,<sup>[20]</sup> interlayer bonding and Li, Na, and Mg migration in ZZ-prismatic and ZZ-octahedral  $\text{Ti}_3\text{C}_2\text{O}_2$  was

investigated. However, neither of these works investigated why the stacking has such a large effect on diffusion, nor how intercalation of ions influences the stability of different stackings. These effects, and the viability of MXenes as intercalation electrodes for Mg, Na, and Li batteries is the focus of this work.

## 2. Simulation Method

The calculations were performed with plane wave DFT code Vienna Ab Initio Simulation Package (VASP, version 5.4.4).<sup>[23–25]</sup> A cut-off of 500 eV was used, with GGA type PBEsol<sup>[26]</sup> functional, described with the projector augmented wave method (PAW).<sup>[27]</sup> The functionals used were the same as used by the Materials Project,<sup>[28]</sup> namely Li\_sv(3), Na\_pv(7), Mg\_pv(8), Ti\_pv(11), H(1), C(4), O(6), F(7), with the number of electrons given in parenthesis. D3 vdW-corrections<sup>[29]</sup> were used, based on the work of Thygesen et al.<sup>[22]</sup> Forces were converged to less than 0.01 eV Å<sup>-1</sup>, with the conjugate gradient method, unless stated otherwise. k-points were generated with the Monkhorst Pack method. The number of k-points used depended on the stacking and on the type of calculation. 12 × 12 k-points were used in the ab-plane for the simulation cells shown in Figure 1. 2, 4, 4, and 8 k-points were used along the c-axis for

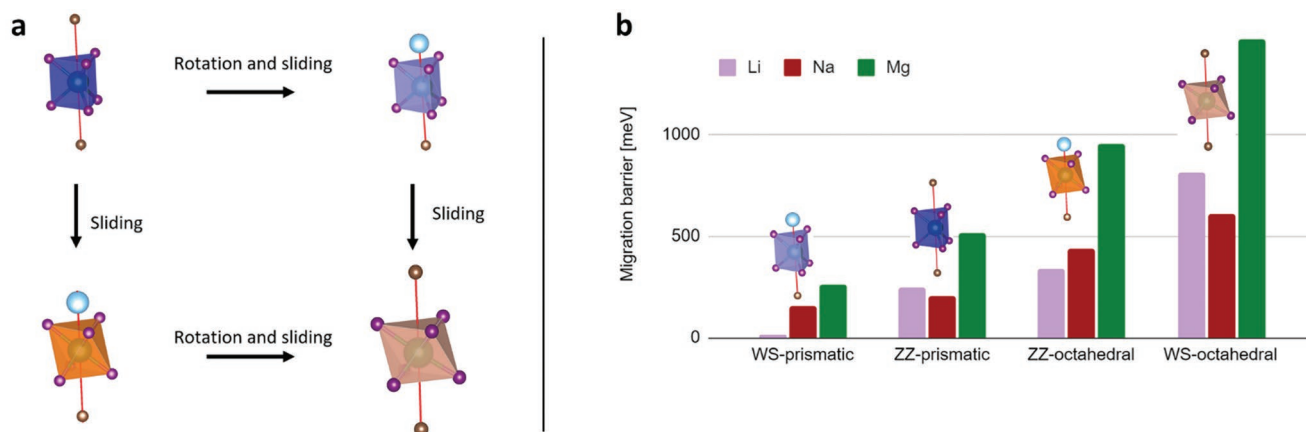


**Figure 2.** a) Schematic illustration showing how the Ti<sub>3</sub>C<sub>2</sub>T<sub>2</sub> stackings in Figure 1d–g) can transition from one to another. Going from ZZ-type stacking to WS-type stacking will require 180° rotations of every other layer to break the zig zag pattern, in addition to sliding of the layers. Going from prismatic type to octahedral type is however possible by only sliding of the layers. b) The migration barriers for Li/Na/Mg ions intercalated in Ti<sub>3</sub>C<sub>2</sub>T<sub>2</sub> stacked in these four different ways.

the WS-octahedral, ZZ-octahedral, ZZ-prismatic, and WS -octahedral stackings, respectively. These simulations were used for generating results shown in Figure 4. For the calculations in Table 2,  $6 \times 6 \times 4$  k-points were used on a simulation cell consisting of  $2 \times 2$  unit cells in the ab-plane. For the Li, Na, and Mg metal references used to calculate voltages included in Figure 4,  $10 \times 10 \times 10$  k-points were used for Li and Na, while  $12 \times 8 \times 8$  k-points were used for Mg. The simulation cells for Li and Na contained two atoms and were body centered cubic structure, while Mg's simulation cell was hexagonal close packed with an orthogonal simulation cell containing four atoms. Partial occupancies were accounted for with the Methfessel–Paxton<sup>[30]</sup> scheme with a smearing width of 0.1 eV. The H<sub>2</sub> reference used in Figure 4 was calculated with one k-point, for a single H<sub>2</sub> molecule in a  $22 \times 22 \times 22$  Å simulation cell. The voltages in Figure 4 were calculated by subtracting zero Kelvin DFT-energies for the products from the reactants, and dividing by two for the case of the divalent Mg. The energy giving relative stability in Figure 4 for a given stacking was calculated in the following way:  $E_{\text{relative stability}} = E_{\text{given stacking}} - E_{\text{least stable stacking}} + 0.1$ , where 0.1 is added simply so that the least stable stacking also will be visible in the plot. All the energies are for one formula unit, i.e., Ti<sub>3</sub>C<sub>2</sub>O<sub>2</sub>. Li/Na/Mg ions were tested in trigonal prismatic, octahedral, and tetrahedral sites between the MXene layers, and the sites with lowest energies (visible in Figure 3) were used when calculating the voltages.

Migration barriers were calculated with the climbing image nudged elastic band method (ci-NEB)<sup>[31]</sup> for Li, Na, and Mg migrating through Ti<sub>3</sub>C<sub>2</sub>O<sub>2</sub>. The migration barriers were calculated with  $4 \times 4 \times 1$  k-points, in a simulation cell as shown in Figure S1 (Supporting Information). For all stackings two layers separated by  $\approx 25$  Å vacuum were used. This enabled the WS-octahedral stacking's barriers to be calculated with two instead of three layers. Two Ti atoms in the center of each MXene layer were locked in the ab-plane, to prevent sliding of adjacent layers, which otherwise could occur when calculating the highest barriers. The forces were relaxed to less than  $0.01 \text{ eV } \text{Å}^{-1}$  here as well, but with a mixture of the Fast Inertial Relaxation Engine (FIRE) and the conjugate gradient method.

We used two ci-NEB images in addition to the endpoints for all calculations, as shown in Figure 3. For Li in ZZ-prismatic stacking an additional calculation was performed, with five images in addition to the endpoints, to ensure that the site at halfway between the energy minima was indeed metastable, despite this being hard to see in Figure 3. The five-image calculation gave the same barrier as the two-image calculation and can be found in the accompanying simulation data. The atomic figures were visualized with VESTA.<sup>[32]</sup>

### 3. Results and Discussion

A total of 12 migration barriers were calculated with DFT for Li, Na, and Mg dilute limit migration in Ti<sub>3</sub>C<sub>2</sub>O<sub>2</sub> stacked in four different ways, see Figure 1. Two of the stackings are as previously mentioned called ZZ-stackings due to their characteristic zig zag pattern. The two other stackings got the prefix WS for whip stitch, as they exhibit a whip stitch pattern. The transitions between the stackings are shown in Figure 2a). The WS-prismatic stacking is obtained by a combination of sliding every other layer of the ZZ-prismatic stacking  $1/3$  of a unit cell, and a 180° rotation around the *c*-axis, obtaining a simple AA stacking, as opposed to ZZ-prismatic and ZZ-octahedral which are AB type stackings. This rotation breaks the zig-zag pattern characteristic of MAX phases. By only sliding layers relative to each other transitioning between both ZZ- and WS-type prismatic and octahedral stacking is possible. One such example is that an WS-octahedral stacking displaying ABC-stacked layers can be obtained by sliding the layers of WS-prismatic stacking.

Despite no previous discussion on the WS-type stackings, TEM images in the work of Halim et al.<sup>[21]</sup> show that both Ti<sub>3</sub>C<sub>2</sub>T<sub>2</sub> MAX phases and MXenes can have instances of layers stacking in WS-type manner, though ZZ-type stacking seems to be more prevalent in their TEM images. Considering that over 20 different MXenes have been synthesized, and more than 50 predicted to be stable,<sup>[4]</sup> it may be that WS-type stacking is present in MXenes other than Ti<sub>3</sub>C<sub>2</sub>T<sub>2</sub>. Finally, there are non-MAX phase MXene precursors of (MC)<sub>n</sub>[Al(A)]<sub>4</sub>C<sub>3</sub> type,

**Table 1.** The relative diffusion coefficients and migration barriers for Li/Na/Mg in  $\text{Ti}_3\text{C}_2\text{O}_2$ , stacked four different ways. The relative diffusion coefficient for Li with SW-prismatic stacking is set to 1.

	Relative diffusion coefficient, with Li in WS-prismatic stacking set to 1 [-]			Migration barrier [meV]		
	Li	Na	Mg	Li	Na	Mg
WS-prismatic	1	$10^{-2}$	$10^{-4}$	17	159	262
ZZ-prismatic	$10^{-4}$	$10^{-3}$	$10^{-8}$	246	202	517
WS-Octahedral	$10^{-5}$	$10^{-7}$	$10^{-16}$	814	611	1473
ZZ-Octahedral	$10^{-13}$	$10^{-10}$	$10^{-24}$	337	439	956

(M = transition metal, A typically Si or Ge),<sup>[4]</sup> which have a WS-type stacking of the  $\text{M}_{n+1}\text{C}_n$  layers and have been used to make the  $\text{Hf}_3\text{C}_2\text{T}_2$  MXene.<sup>[33]</sup> Unfortunately, TEM images revealing the stacking of non-MAX phase MXenes are not published to the authors knowledge, so it is not known if the WS-stacking in the  $(\text{MC})_n[\text{Al}(\text{A})]_4\text{C}_3$  phase is conserved after etching.

There is a clear trend shown in Figure 2b), with all three ions going from low to high migration barrier when moving from WS-prismatic, via ZZ-prismatic and ZZ-octahedral to WS-octahedral stacking. The difference in migration barriers is significant between the different stackings. Lithium intercalated in WS-prismatic stacking has the lowest barrier at 17 meV, while Mg intercalated in WS-octahedral has the highest barrier at 1470 meV. This implies 24 orders of magnitude difference in diffusion coefficient for the two cases, at a temperature of 298 K and assuming that the diffusion is proportional to  $\exp(-E_B/k_B T)$ , where  $E_B$  is the migration barrier,  $k_B$  is the boltzmann constant, and  $T$  is the absolute temperature. The relative diffusion of ions in the differently stacked  $\text{Ti}_3\text{C}_2\text{O}_2$  (compared with Li in WS prismatic stacking) is shown in Table 1, together with the migration barrier. It is evident that the stacking and the resulting coordination is critical when considering diffusion of ions in MXenes.

Canepa et al.<sup>[7]</sup> presented a rough estimate on how high a migration barrier can be for Mg electrodes. Neglecting all kinetics except intra particle diffusion and assuming 1  $\mu\text{m}$  spherical particles at 25 °C, a barrier of 500 meV should allow a C-rate of 1. A C-rate of 1 means that the electrode can be charged/discharged in 1 h. A later work with Canepa as co-author presents a very similar model,<sup>[34]</sup> and lists a maximum tolerable migration barrier of 600 meV for 1  $\mu\text{m}$  particles at an elevated temperature of 60 °C. It is evident from Table 1 that the octahedral stackings are unsuitable for Mg intercalation, while the WS-prismatic is within a reasonable range. From Figure 2 and Table 1 is clear that stacking is as important as the ionic species for the diffusion kinetics. With the right stacking and coordination for Mg, it can have as fast diffusion as Li coordinated in an unfavorable way (e.g., Mg in SW-prismatic vs Li in SW-Octahedral stacking).

Another takeaway would be that Mg has  $10^2$  to  $10^{14}$  slower migration than Li and Na, depending on stacking. A key question is why the migration barriers depend so much on the stacking. To better understand this, the coordination for the ions at different points in the barriers were evaluated and are shown in Figure 3. For the ZZ-prismatic stacking, the minimum energy site (at 0 and 1 on the  $x$ -axis in the plots) is between two carbon atoms, coordinated in a trigonal prismatic

way by the oxygen termination groups. The transition state is where the ion travels through one of the faces of the prism, giving a square planar coordination. Then there is a metastable site (halfway along the migration path) with trigonal prismatic coordination again, but this time the intercalated ion resides between two titanium atoms. To get back to the minimum energy site, the ion must move through a square planar face again, giving the symmetry of the migration energy profile.

There are several details worth noticing for this migration path for the ZZ-prismatic stacking. First is the energy difference between the minimum energy site and the metastable site. Both sites have the same trigonal prismatic coordination. But despite this, there is an energy difference between these two sites for all ions. It may seem like unfavorable columbic repulsion between the intercalated ions and the positively charged Ti can destabilizes the metastable site quite significantly for the ZZ-prismatic stacking. Supporting this argument, is the fact that the WS prismatic stacking has no metastable site halfway along the  $x$ -axis. This can be explained by there being an equal destabilizing effect from one positive Ti atom both at start/end of the migration path and midway. There is still an energy barrier to overcome in the WS-prismatic stacking when ions go through square planar coordination when moving from at start to midway. This energy barrier is however small compared to the energy differences between the stable and metastable site for all other stackings, especially for Li.

A similar trend with destabilization from the presence of Ti can be seen for the octahedral stackings. The relative stability of the tetrahedral site at halfway along the migration path to the octahedral site at the beginning in Figure 3 seems to be the most important parameter for the migration barrier. For the ZZ-octahedral stacking, the minimum energy site is destabilized by a positive Ti atom, while the tetrahedral site may have a stabilizing effect from the negative carbide atom. For the WS-octahedral stacking however, the minimum energy site is stabilized by two carbide atoms, while there is nothing stabilizing the tetrahedral site. This trend and migration path can resemble the case for spinel type electrode materials, where investigations have shown that the relative stability of the tetrahedral and the octahedral site is key to obtaining fast diffusion.<sup>[35,36]</sup>

Worth noticing is that Mg has roughly twice as high migration barriers as Li/Na for all cases. This is as expected, since approximately twice as high coulombic interactions would be expected from intercalated  $\text{Mg}^{2+}$  compared to  $\text{Li}^+/\text{Na}^+$ . Finally, simply looking at coordination number would also suggest that the octahedral stackings have higher migration barriers than the prismatic stackings. One way to view the coordination



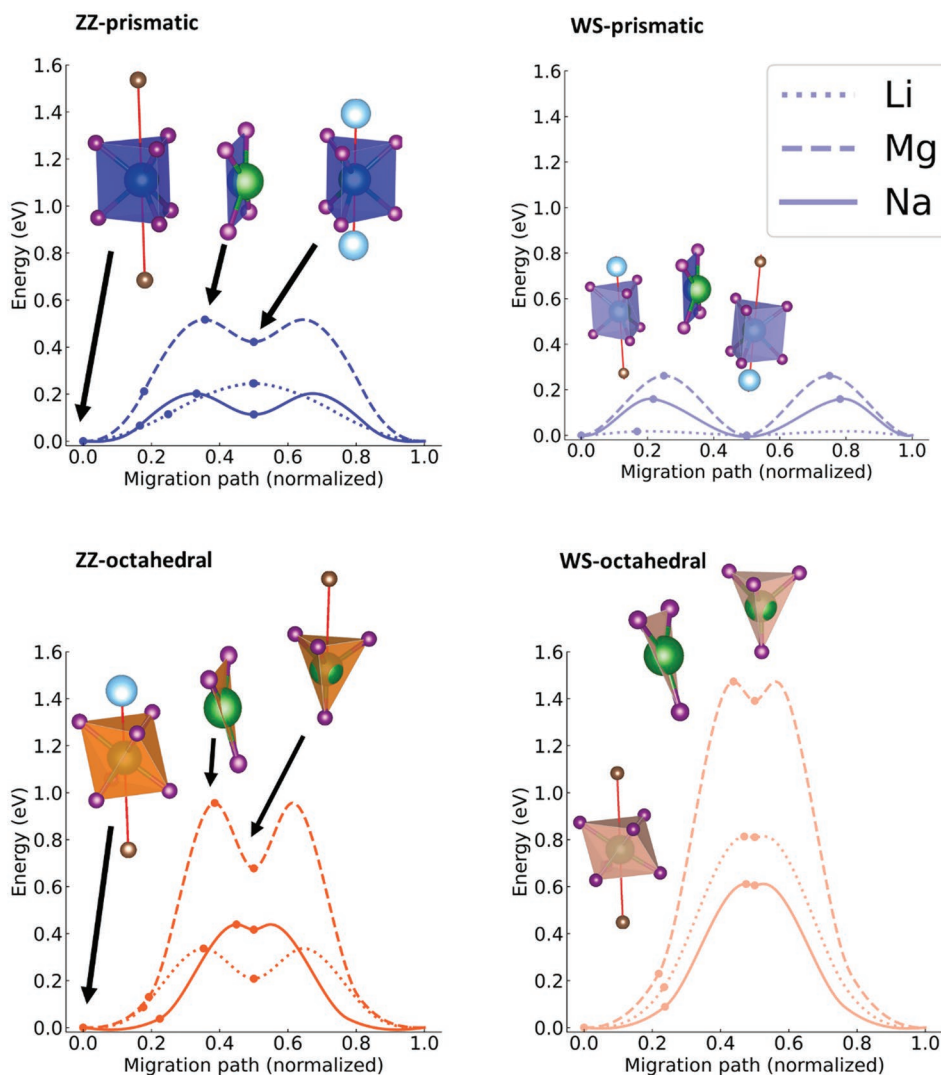


**Figure 3.** The migration barrier profiles for Li, Na, and Mg migrating through  $\text{Ti}_3\text{C}_2\text{O}_2$ -MXene with ZZ-prismatic, WS-prismatic, WS-octahedral, and ZZ-octahedral stacking, given in clockwise order starting top left. The way oxygen coordinates Li/Na/Mg at the minimum energy site (beginning of migration path), Metastable site (halfway along the migration path) and the transition state (energy maxima along the migration path) are included. For ZZ-prismatic stacking with Li the transition state is practically on top of the metastable state. The position of the images used in ci-NEB is shown as round markers.

number is as the number of ionic bonds. For the octahedral stackings the coordination number goes from 6-3-4-3-6 along the transition path in Figure 3. For the prismatic stackings the same path gives 6-4-6-4-6 as the sequence of coordination numbers, suggesting that fewer ionic bonds need to be broken for migration in the prismatic cases, giving lower migration barriers. Thus, these results suggest that materials having neighboring trigonal prismatic sites may be well suited for electrode materials, especially for Mg where sluggish diffusion is a common problem

The relative stability of the different stackings was investigated for  $\text{Ti}_3\text{C}_2\text{T}_2$  with and without intercalated Li/Na/Mg. The results are shown in Figure 4. The results agree with previous reports<sup>[19,20]</sup> for the unintercalated  $\text{Ti}_3\text{C}_2\text{T}_2$ , with the prismatic stackings being most stable for  $\text{Ti}_3\text{C}_2\text{O}(\text{OH})$ . There is no noticeable difference between the ZZ and WS prismatic stackings.

For the octahedral stackings, however, the WS type is slightly more stable for both  $\text{Ti}_3\text{C}_2\text{F}_2$  and  $\text{Ti}_3\text{C}_2\text{O}_2$ , which may be due to the WS-octahedral having all negatively charged termination groups placed adjacent to positively charged Ti atom. Similarly, the ZZ-octahedral is more favorable than the WS-octahedral  $\text{Ti}_3\text{C}_2\text{O}(\text{OH})$ , where unfavorable interaction from positively charged H and adjacent Ti may be present.

When ions intercalate the differences become more pronounced for all stackings. For the WS-prismatic stacking the structure was unstable upon intercalation of ions, displaying strong distortion of both the stacking and the inner MXene structure, and the energies are therefore omitted. The WS-octahedral on the other, proved to be far more stable than the ZZ-octahedral and ZZ-prismatic upon intercalation of the ions. While the ZZ-octahedral stacking proved more stable than the ZZ-prismatic for Li and Mg, but not Na. From just

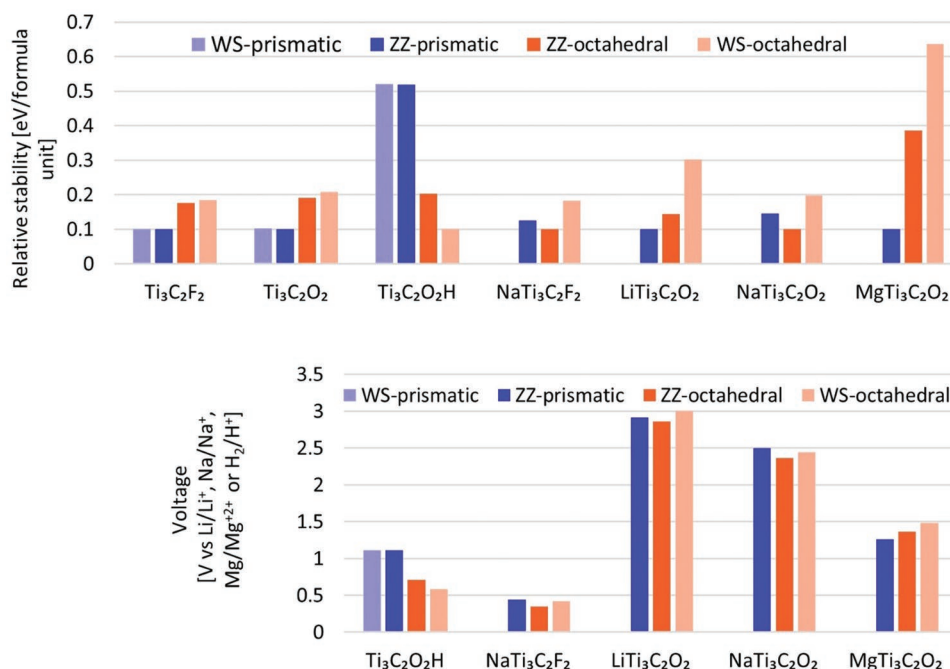


**Figure 4.** The relative stability of different stackings for selected termination groups and Li, Na, and Mg intercalated. The least stable stacking for every termination group chemistry is set to 0.1 eV, and differences in energy between the stackings corresponds to the energy needed to transition from one stacking to another, per formula unit, i.e., per  $\text{LiTi}_3\text{C}_2\text{O}_2$ . WS-prismatic stacking was unstable for several of the compositions, for which cases no bar with WS-prismatic is plotted. The voltages are for Li, Na, and Mg metal reacting with the given MXenes, i.e.,  $\text{Ti}_3\text{C}_2\text{O}_2 + \text{Mg} \rightarrow \text{MgTi}_3\text{C}_2\text{O}_2$ . This would correspond to the average voltage when going from 0% to 100% Li/Na/Mg intercalation. The  $\text{Ti}_3\text{C}_2\text{O}_2\text{H}$  voltage is for the reaction  $\text{Ti}_3\text{C}_2\text{O}_2 + \frac{1}{2} \text{H}_2 \rightarrow \text{Ti}_3\text{C}_2\text{O}(\text{OH})$ .

considering coulombic interactions between O and Na, the octahedral stacking should be the one with lowest energy, as octahedral coordination allows for the smallest  $\text{Na}^+ - \text{O}^{2-}$  distance, and the largest  $\text{O}^{2-} - \text{O}^{2-}$  distance, optimizing favorable coulombic interactions. ZZ-prismatic stacking does however have a more favorable position of C and Ti in the structure compared to ZZ-octahedral, and it may be that this outweighs the coulombic interactions in favor of octahedral coordination for Na. Na-preference for trigonal ZZ-prismatic does resemble trends in other layered materials where Na is known to have a preference for trigonal prismatic coordination under some conditions.<sup>[37]</sup>

For Li and especially Mg there is a preference for the octahedral stackings. As more Li/Mg is intercalated it is more likely that an octahedral stacking with slow diffusion will be energetically favored. It is also worth noting that the WS-octahedral stacking is significantly more stable than other stackings upon intercalation, suggesting that the characteristic zig-zag pattern of the MAX-phases is only metastable for  $\text{Ti}_3\text{C}_2\text{O}_2$  with intercalated Li/Mg. For Li the decrease in diffusion from ZZ-prismatic to ZZ-octahedral is only tenfold, as can be seen in Table 1. For Mg the difference between ZZ-prismatic and ZZ-octahedral is eight orders magnitude. Thus, it seems Mg intercalation in  $\text{Ti}_3\text{C}_2\text{O}_2$  is only possible with prismatic stacking. As the Mg intercalated  $\text{Ti}_3\text{C}_2\text{O}_2$ , i.e.,  $\text{MgTi}_3\text{C}_2\text{O}_2$ , has a strong preference for the octahedral stackings with poor diffusion properties, it seems hard to imagine purely oxygen terminated  $\text{Ti}_3\text{C}_2\text{O}_2$  MXene cathodes for Mg batteries. However, a natural question is whether the ZZ-prismatic stacking with fast diffusion can be stabilized with Mg intercalated.

One way to stabilize the ZZ-prismatic stacking would be to have stabilization from OH-termination groups, as Figure 4 shows that the 50% OH-terminated  $\text{Ti}_3\text{C}_2\text{O}(\text{OH})$  has a strong preference for ZZ-prismatic stacking. To investigate this possibility, the relative stability of Li/Na/Mg<sub>0.25</sub> $\text{Ti}_3\text{C}_2\text{O}(\text{OH})$ , Li/Na/Mg<sub>0.5</sub> $\text{Ti}_3\text{C}_2\text{O}(\text{OH})$ , Li/Na/Mg<sub>0.75</sub> $\text{Ti}_3\text{C}_2\text{O}(\text{OH})$ , and Li/Na/Mg $\text{Ti}_3\text{C}_2\text{O}(\text{OH})$ , in ZZ prismatic and octahedral stacking was calculated. The results, given in Table 2, shows that

**Table 2.** The stability of Li/Na/Mg<sub>x</sub> $\text{Ti}_3\text{C}_2\text{O}(\text{OH})$  with ZZ-prismatic and ZZ-octahedral type stacking. Unstable denotes that  $\text{H}_2$  formed, the layers separated, or that the MXene structure decomposed in some other way. The energies can be found in the Supporting Information.

	ZZ-prismatic	ZZ-octahedral
$\text{Li}_{0.25}\text{Ti}_3\text{C}_2\text{O}(\text{OH})$	Stable	Metastable
$\text{Li}_{0.5}\text{Ti}_3\text{C}_2\text{O}(\text{OH})$	Stable	Metastable
$\text{Li}_{0.75}\text{Ti}_3\text{C}_2\text{O}(\text{OH})$	Stable	Metastable
$\text{LiTi}_3\text{C}_2\text{O}(\text{OH})$	Stable	Metastable
$\text{Na}_{0.25}\text{Ti}_3\text{C}_2\text{O}(\text{OH})$	Stable	Metastable
$\text{Na}_{0.5}\text{Ti}_3\text{C}_2\text{O}(\text{OH})$	Metastable	Stable
$\text{Na}_{0.75}\text{Ti}_3\text{C}_2\text{O}(\text{OH})$	Stable	Metastable
$\text{NaTi}_3\text{C}_2\text{O}(\text{OH})$	Metastable	Unstable
$\text{Mg}_{0.25}\text{Ti}_3\text{C}_2\text{O}(\text{OH})$	Stable	Metastable
$\text{Mg}_{0.5}\text{Ti}_3\text{C}_2\text{O}(\text{OH})$	Metastable	Stable
$\text{Mg}_{0.75}\text{Ti}_3\text{C}_2\text{O}(\text{OH})$	Unstable	Unstable
$\text{MgTi}_3\text{C}_2\text{O}(\text{OH})$	Unstable	Unstable

ZZ-prismatic is only stable for 25% Mg intercalated, in contrast to Na and especially Li which shows much larger stability for ZZ-prismatic. This suggests that it may only be possible to intercalate small amounts of Mg if the ZZ-prismatic structure is to be stable, despite the stabilization from OH-termination.

This does however assume that the migration barriers of Mg are not increased significantly by the presence of OH. Also worth mentioning is that the capacity is reduced by at least 50% if at most 50% Mg can be intercalated. Further, the voltage of  $\text{MgTi}_3\text{C}_2\text{O}(\text{OH})$  is considerably lower than that of  $\text{MgTi}_3\text{C}_2\text{O}_2$ , further decreasing the prospects of  $\text{Ti}_3\text{C}_2\text{T}_2$  as a cathode material in Mg batteries. Finally, proton (de)intercalation is a common problem with Mg batteries,<sup>[5]</sup> and there could be the problem of  $\text{H}^+$  de-intercalating instead of Li/Na/Mg when cycling. Figure 4 shows that energetically the deintercalation of  $\text{H}^+$  through the reaction  $\text{Ti}_3\text{C}_2\text{O}(\text{OH}) \rightarrow \text{Ti}_3\text{C}_2\text{O}_2 + \frac{1}{2} \text{H}_2$  is preferred over the deintercalation Li/Na/Mg. Finally, there is the possibility of a more fluoride terminated surface. However, fluoride terminated  $\text{Ti}_3\text{C}_2\text{T}_2$  have been shown to favor octahedral type stackings,<sup>[20]</sup> and has also shown instability when fully intercalated as in the case of  $\text{MgTi}_3\text{C}_2\text{F}_2$ .<sup>[3]</sup> So  $\text{Ti}_3\text{C}_2\text{T}_2$  does not seem to be a promising cathode material for Mg batteries with neither O, F, nor OH-termination.

As previously mentioned has  $\text{Ti}_3\text{C}_2\text{T}_2$  been investigated for use as anodes with both Li and Na.<sup>[1,2]</sup> Especially for Na-ion batteries, where graphite cannot be utilized as anode material,<sup>[38]</sup> a MXene anode may be of great interest.  $\text{NaTi}_3\text{C}_2\text{F}_2$  was therefore included in Figure 4, and it shows the same trend as  $\text{NaTi}_3\text{C}_2\text{O}_2$  with the ZZ-prismatic stacking being preferred. The voltage obtained is however much lower, which would be beneficial for anode applications. The migration barriers for  $\text{Ti}_3\text{C}_2\text{F}_2$  would also be expected to be significantly lower than the already low barriers for Na in  $\text{Ti}_3\text{C}_2\text{O}_2$ , as the columbic interactions would be considerably weaker with singly charged  $\text{F}^-$  compared to  $\text{O}^{2-}$ . Promising results have already been achieved for  $\text{Ti}_3\text{C}_2\text{T}_x$  anodes for Na applications,<sup>[2]</sup> but to further improve them, emphasis on termination group chemistry and stacking should be made, to get the best stacking with the lowest migration barriers and an optimal voltage.

The WS-prismatic stacking is interesting from a theoretical point of view, as it shows that extremely low migration barriers are possible even for Mg in oxide cathodes. Despite that the stacking is unstable upon intercalation for  $\text{Ti}_3\text{C}_2\text{O}_2$ , the favorable Li/Na/Mg coordination giving the low migration barriers might exist for other materials which are stable. There are also other MXenes worth exploring.  $\text{Mo}_2\text{CO}_2$  MXene for instance is predicted<sup>[39]</sup> to have the termination groups placed differently than  $\text{Ti}_3\text{C}_2\text{O}_2$ , which would make the stability of the different sites for intercalants play out differently.  $\text{V}_2\text{CT}_x$  has been predicted to give quite different voltages than  $\text{Ti}_3\text{C}_2\text{O}_2$ , and lower migration barriers due to weaker ionic interactions with intercalants.<sup>[3]</sup> Thus, further exploration of the MXene space is needed to truly understand the viability of MXene electrodes.

## 4. Conclusion

$\text{Ti}_3\text{C}_2\text{T}_2$  stacked in four different ways was investigated with respect to stability and intercalation properties for Li, Na, and

Mg. It was demonstrated that an optimal stacking can reduce the diffusion by up to 20 orders of magnitude for  $\text{Ti}_3\text{C}_2\text{O}_2$ . The reason for this appears to be from both the different ways oxygen coordinates Li/Na/Mg during migration, and from the (de)stabilizing effect on the transition states from Ti and C ions in the MXene layers. The trend indicates that stackings associated with slow diffusion were the most thermodynamically stable ones, with the ABC-stacked WS-octahedral stacking being by far the most stable upon intercalation. The prospect of using  $\text{Ti}_3\text{C}_2\text{O}_2$  for Mg battery cathode applications was considered and found to be challenging, as Mg showed the strongest preference for the stackings giving prohibitively slow diffusion. Na on the other hand displayed some preference for the fast diffusion stackings, and  $\text{Ti}_3\text{C}_2\text{O}_2$  and/or  $\text{Ti}_3\text{C}_2\text{F}_2$  were considered as good electrode candidates for Na.

## Supporting Information

Supporting Information is available from the Wiley Online Library or from the author.

## Acknowledgements

The computations were performed on resources provided by UNINETT Sigma2 – the National Infrastructure for High Performance Computing and Data Storage in Norway with Project No. NN9414K.

## Conflict of Interest

The authors declare no conflict of interest.

## Author Contributions

J.H.-J. conceived the concept and performed the simulations. Both authors contributed to the writing of the article.

## Data Availability Statement

The data that support the findings of this study are openly available in zenodo.org at [https://urldefense.com/v3/\\_\\_http://doi.org/10.5281/zenodo.5392560\\_\\_;!!N11eV2iwtfs!uiaU8YP\\_TeMcnRzdCy8v9\\_iXbDF6dPjQcsmGELdmWj5fk6wbw-l\\_5A8U1bb7onphWjxO6ydbkrUqZs3a77dAalyFf6L\\_otEm\\$](https://urldefense.com/v3/__http://doi.org/10.5281/zenodo.5392560__;!!N11eV2iwtfs!uiaU8YP_TeMcnRzdCy8v9_iXbDF6dPjQcsmGELdmWj5fk6wbw-l_5A8U1bb7onphWjxO6ydbkrUqZs3a77dAalyFf6L_otEm$), reference number 10.5281/zenodo.5392560.

## Keywords

battery technology, energy storage, MXene, stacking order

Received: January 3, 2022

Revised: March 17, 2022

Published online:

[1] R. Cheng, T. Hu, H. Zhang, C. Wang, M. Hu, J. Yang, C. Cui, T. Guang, C. Li, C. Shi, P. Hou, X. Wang, *J. Phys. Chem. C* **2019**, 123, 1099.

[2] X. Wang, X.i Shen, Y. Gao, Z. Wang, R. Yu, L. Chen, *J. Am. Chem. Soc.* **2015**, 137, 2715.

- [3] H. Kaland, J. Hadler-Jacobsen, F. H. Fagerli, N. P. Wagner, Z. Wang, S. M. Selbach, F. Vullum-Bruer, K. Wiik, S. K. Schnell, *Sustainable Energy Fuels* **2020**, *4*, 2956.
- [4] B. Anasori, Y. Gogotsi, *2D Metal Carbides and Nitrides (MXenes)*, Vol. 2, Springer Nature, Cham **2019**.
- [5] I. D. Johnson, B. J. Ingram, J. Cabana, *ACS Energy Lett.* **2021**, *6*, 1892.
- [6] Y. Liang, H. Dong, D. Aurbach, Y. Yao, *Nat. Energy* **2020**, *5*, 646.
- [7] P. Canepa, G. Sai Gautam, D. C. Hannah, R. Malik, M. Liu, K. G. Gallagher, K. A. Persson, G. Ceder, *Chem. Rev.* **2017**, *117*, 4287.
- [8] M. Xu, M. G. Soliman, X. Sun, B. Pelaz, N. Feliu, W. J. Parak, S. Liu, *ACS Nano* **2018**, *12*, 10104.
- [9] J. Zhu, R. Shi, Y. Liu, Y. Zhu, J. Zhang, X. Hu, L. Li, *Appl. Surf. Sci.* **2020**, *528*, 146985.
- [10] M.-Q. Zhao, C. E. Ren, M. Alhabeab, B. Anasori, M. W. Barsoum, Y. Gogotsi, *ACS Appl. Energy Mater.* **2019**, *2*, 1572.
- [11] H. Dong, Y. Liang, O. Tutusaus, R. Mohtadi, Y. Zhang, F. Hao, Y. Yao, *Joule* **2019**, *3*, 782.
- [12] H.-W. Wang, M. Naguib, K. Page, D. J. Wesolowski, Y. Gogotsi, *Chem. Mater.* **2016**, *28*, 349.
- [13] P. O. Å. Persson, J. Rosen, *Curr. Opin. Solid State Mater. Sci.* **2019**, *23*, 100774.
- [14] V. Kamysbayev, A. S. Filatov, H. Hu, X. Rui, F. Lagunas, D. Wang, R. F. Klie, D. V. Talapin, *Science* **2020**, *369*, 979.
- [15] J. Lu, I. Persson, H. Lind, J. Palisaitis, M. Li, Y. Li, K. Chen, J. Zhou, S. Du, Z. Chai, Z. Huang, L. Hultman, P. Eklund, J. Rosen, Q. Huang, P. O. Å. Persson, *Nanoscale Adv.* **2019**, *1*, 3680.
- [16] M. Naguib, J. Halim, J. Lu, K. M. Cook, L. Hultman, Y. Gogotsi, M. W. Barsoum, *J. Am. Chem. Soc.* **2013**, *135*, 15966.
- [17] Y. Xie, M. Naguib, V. N. Mochalin, M. W. Barsoum, Y. Gogotsi, X. Yu, K.-W. Nam, X.-Q. Yang, A. I. Kolesnikov, P. R. C. Kent, *J. Am. Chem. Soc.* **2014**, *136*, 6385.
- [18] T. Hu, H. Zhang, J. Wang, Z. Li, M. Hu, J. Tan, P. Hou, F. Li, X. Wang, *Sci. Rep.* **2015**, *5*, 16329.
- [19] T. Hu, M. Hu, Z. Li, H. Zhang, C. Zhang, J. Wang, X. Wang, *Phys. Chem. Chem. Phys.* **2016**, *18*, 20256.
- [20] J. Hadler-Jacobsen, F. H. Fagerli, H. Kaland, S. K. Schnell, *ACS Mater. Lett.* **2021**, *3*, 1369.
- [21] J. Halim, M. R. Lukatskaya, K. M. Cook, J. Lu, C. R. Smith, L.-Å. Näslund, S. J. May, L. Hultman, Y. Gogotsi, P. Eklund, M. W. Barsoum, *Chem. Mater.* **2014**, *26*, 2374.
- [22] A. S. Tygesen, M. Pandey, T. Vegge, K. S. Thygesen, J. M. García-Lastra, *J. Phys. Chem. C* **2019**, *123*, 4064.
- [23] G. Kresse, J. Furthmüller, *Phys. Rev. B* **1996**, *54*, 11169.
- [24] G. Kresse, J. Furthmüller, *Comput. Mater. Sci.* **1996**, *6*, 15.
- [25] G. Kresse, J. Hafner, *Phys. Rev. B* **1994**, *49*, 14251.
- [26] G. I. Csonka, J. P. Perdew, A. Ruzsinszky, P. H. T. Philipsen, S. Lebègue, J. Paier, O. A. Vydrov, J. G. Ángyán, *Phys. Rev. B: Condens. Matter Mater. Phys.* **2009**, *79*, 155107.
- [27] D. Joubert, *Phys. Rev. B: Condens. Matter Mater. Phys.* **1999**, *59*, 1758.
- [28] A. Jain, S. P. Ong, G. Hautier, W. Chen, W. D. Richards, S. Dacek, S. Cholia, D. Gunter, D. Skinner, G. Ceder, K. A. Persson, *APL Mater.* **2013**, *1*, 011002.
- [29] S. Grimme, J. Antony, S. Ehrlich, H. Krieg, *J. Chem. Phys.* **2010**, *132*, 154104.
- [30] M. Methfessel, A. T. Paxton, *Phys. Rev. B* **1989**, *40*, 3616.
- [31] G. Henkelman, B. P. Uberuaga, H. Jónsson, *J. Chem. Phys.* **2000**, *113*, 9901.
- [32] K. Momma, F. Izumi, *J. Appl. Crystallogr.* **2011**, *44*, 1272.
- [33] J. Zhou, X. Zha, X. Zhou, F. Chen, G. Gao, S. Wang, C. Shen, T. Chen, C. Zhi, P. Eklund, S. Du, J. Xue, W. Shi, Z. Chai, Q. Huang, *ACS Nano* **2017**, *11*, 3841.
- [34] T. Chen, G. Sai Gautam, P. Canepa, *Chem. Mater.* **2019**, *31*, 8087.
- [35] Z. Rong, R. Malik, P. Canepa, G. Sai Gautam, M. Liu, A. Jain, K. Persson, G. Ceder, *Chem. Mater.* **2015**, *27*, 6016.
- [36] X. Sun, P. Bonnick, V. Duffort, M. Liu, Z. Rong, K. A. Persson, G. Ceder, L. F. Nazar, *Energy Environ. Sci.* **2016**, *9*, 2273.
- [37] J. C. Kim, D.-H. Kwon, J. H. Yang, H. Kim, S.-H. Bo, L. Wu, H. Kim, D.-H. Seo, T. Shi, J. Wang, Y. Zhu, G. Ceder, *Adv. Energy Mater.* **2020**, *10*, 2001151.
- [38] Y. Tian, G. Zeng, A. Rutt, T. Shi, H. Kim, J. Wang, J. Koettgen, Y. Sun, B. Ouyang, T. Chen, Z. Lun, Z. Rong, K. Persson, G. Ceder, *Chem. Rev.* **2021**, *121*, 1623.
- [39] M. Khazaei, M. Arai, T. Sasaki, M. Estili, Y. Sakka, *Phys. Chem. Chem. Phys.* **2014**, *16*, 7841.